ChemPubSoc Europe

DOI: 10.1002/chem.201304063

CHEMISTRY
A European Journal
Full Paper

Magnetic Resonance Imaging

Comprehensive Evaluation of the Physicochemical Properties of Ln^{III} Complexes of Aminoethyl-DO3A as pH-Responsive T_1-MRI Contrast Agents**

Zsolt Baranyai,[a] Gabriele A. Rolla,[b] Roberto Negri,[c] Attila Forgács,[a] Giovanni B. Giovenzana,*[c] and Lorenzo Tei*[b]

Abstract: *N*-Substituted aminoethyl groups were attached to 1,4,7,10-tetraazacyclododecane-1,4,7-triacetic acid (DO3A) with the aim to design pH-responsive Ln^{III} complexes based on the pH-dependent on/off ligation of the amine nitrogen to the metal ion. The following ligands were synthesized: **AE-DO3A** (aminoethyl-DO3A), **MAE-DO3A** (*N*-methylaminoethyl-DO3A), **DMAE-DO3A** (*N*,*N*-dimethylaminoethyl-DO3A) and **MEM-AE-DO3A** (*N*-methoxyethyl-*N*-methylaminoethyl-DO3A). The physicochemical properties of the Ln^{III} complexes were investigated for the evaluation of their potential applicability as magnetic resonance imaging (MRI) contrast agents. In particular, a ^{1}H and ^{17}O NMR relaxometric study was carried out for these Gd^{III} complexes at two different pH values: at basic pH (pendant amino group coordinated to the metal centre) and at acidic pH (protonated amine, not interacting with the metal ion). Eu^{III} complexes allow one to estimate the number of inner-sphere water molecules through luminescence lifetime measurements and obtain some structural information through variable-temperature (VT) high-resolution ^{1}H NMR studies. Equilibria between differently hydrated species were found for most of the complexes at both acidic and basic pH. The thermodynamic stability of Ca^{II}, Zn^{II}, Cu^{II} and Ln^{III} complexes and kinetics of formation and dissociation reactions of Ln^{III} complexes of **AE-DO3A** and **DMAE-DO3A** were investigated showing stabilities comparable to currently approved Gd^{III}-based CAs. In detail, higher total basicity ($\Sigma \log K_i^H$) and higher stability constants of Ln^{III} complexes were found for **AE-DO3A** with respect to **DMAE-DO3A** (i.e., $\log K_{\text{Gd-AE-DO3A}} = 22.40$ and $\log K_{\text{Gd-DMAE-DO3A}} = 20.56$). The transmetallation reactions of Gd^{III} complexes are very slow (Gd-**AE-DO3A**: $t_{1/2} = 2.7 \times 10^4$ h; Gd-**DMAE-DO3A**: 1.1×10^5 h at pH 7.4 and 298 K) and occur through proton-assisted dissociation.

Introduction

MRI diagnostics takes advantage of specific contrast agents (CAs) to improve the quality of the registered image.[1] Two families of contrast agents, namely paramagnetic chelates and superparamagnetic nanoparticles have been used in the last three decades as T_1 and T_2 CAs, respectively, and a detailed knowledge of their potentiality has been gained. Paramagnetic CAs operate by reducing the longitudinal relaxation time (T_1) of water protons, leading to a local brightening of the image; the ability to reduce T_1 is measured by a parameter called relaxivity (r_{1p}). The relaxivity of a paramagnetic metal complex is dependent on several parameters, and can be improved by: 1) slowing the rotational motion of the paramagnetic centre encasing the latter in a large molecule (typically by covalent- or non-covalent binding to physiological or synthetic biocompatible macromolecules);[2] 2) increasing the number (q) of water molecules directly coordinated to the metal ion and their rate of exchange with bulk water;[3] 3) improving the local concentration of paramagnetic metal centres, linking the single chelates in multimeric systems[4] or collecting them in well-defined nanoparticles.[5]

The chemistry of paramagnetic complexes is well summarized in dedicated reviews[6] and books,[7] and the results of the activity in this field is witnessed by hundreds of derivatives, devised to optimize the chemical and magnetic properties.[8] The observation of toxic effects related to long term dissociation[9] of the metal ion from the corresponding complex prompted research efforts aimed at the enhancement of both the thermodynamic and kinetic stability of the chelates, generally tackled by structural reinforcement of the ligand structures.[10] The

[a] *Dr. Z. Baranyai, A. Forgács*
Department of Inorganic and Analytical Chemistry
University of Debrecen, H-4010 Debrecen Egyetem tér 1 (Hungary)

[b] *Dr. G. A. Rolla, Dr. L. Tei*
Dipartimento di Scienze e Innovazione Tecnologica
Università del Piemonte Orientale "Amedeo Avogadro"
Viale T. Michel 11, 15121 Alessandria (Italy)
E-mail: lorenzo.tei@mfn.unipmn.it

[c] *Dr. R. Negri, Prof. G. B. Giovenzana*
Dipartimento di Scienze del Farmaco
Università del Piemonte Orientale "Amedeo Avogadro"
Largo Donegani 2/3, 28100 Novara (Italy)
E-mail: giovenzana@pharm.unipmn.it

[**] *DO3A = 1,4,7,10-tetraazacyclododecane-1,4,7-triacetic acid*

Supporting information for this article is available on the WWW under http://dx.doi.org/10.1002/chem.201304063.

recent development of molecular imaging applications,[11] in which imaging probes are required to report specific changes in physical or (bio)chemical parameters led to an extensive research for "responsive" MRI probes. Recent reviews summarize the wide array of responsive paramagnetic chelates, designed to monitor different parameters such as pH,[12] pO_2,[13] the concentration of glucose,[14] metal ions[15] and enzymes.[16] pH represents one of the first and most important targets: significant variations from physiological values may be associated with a number of pathologies, cancer being the most representative.[17] Several different pH-sensitive CAs were reported in the scientific literature. Gd-based CAs usually rely on the variation of number of inner-sphere water molecules (q)[18] or reorientational correlation time (τ_R)[19] to obtain a pH-dependent behaviour. PARACEST agents[20] show a large pH sensitivity elicited by a mechanism involving chemical exchange of amide protons of the paramagnetic complex.[21] Among the Gd-based CAs, a macrocyclic DO3A-like system embodying a β-sulfonamidoethyl group (Gd-**DO3A**-**SA**)[18] represents a prototypical example of the strategy involving the modulation of the coordination to affect the relaxivity of the complex. The deprotonation of the sulfonamide in the side arm triggers the coordination of the metal by this donor group, replacing coordinated water molecules. We have recently reported a versatile extension of this interesting reversible mechanism, by using a ligand bearing a side arm containing a simple amino group, whose protonation/deprotonation leads to a modification of the corresponding complex structure and dynamics. The simple amino group allows us to finely modulate the pK of this change by N-substitution with suitable alkyl groups.[22] Recently, the pH-dependent PARACEST effect of the Eu^{III} complex with amino- and dimethylaminoethyl-DO3As has been reported showing an additional interesting application of this class of ligands.[23]

Herein we report a comprehensive evaluation of physicochemical properties of selected Ln^{III} complexes of aminoethyl-DO3As, relevant to their potential application as MRI contrast agents, and highlighting the key role of *N*-alkyl substituents on the solution structure and dynamics of the corresponding complexes.

Results and Discussion

Synthesis

The aminoethyl-functionalized DO3A-like ligands employed for the formation of paramagnetic complexes of this work are depicted in Scheme 1. The ligand **AE-DO3A** (aminoethyl-DO3A) represents the parent (N-unsubstituted) compound of this series. Substitution with simple methyl groups leads to **MAE-DO3A** (*N*-methylaminoethyl-DO3A) and **DMAE-DO3A** (*N*,*N*-dimethylaminoethyl-DO3A), designed to explore the effect of the sequential substitution on the exocyclic nitrogen atom. The fourth ligand (**MEM-AE-DO3A**, *N*-methoxyethyl-*N*-methylaminoethyl-DO3A) has a tertiary amino group in which one of the N-substituents carries an additional weak donor atom (ether oxygen), devised to gain a supplementary influence on the metal coordination sphere, with the side arm acting as potential bidentate, although maintaining the overall basicity profile of the ligand family.

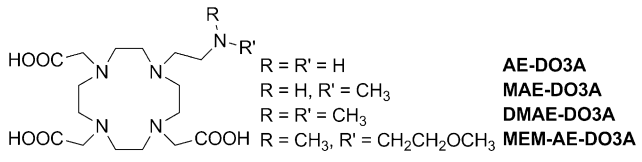

Scheme 1. Aminoethyl-functionalized **DO3A** complexes.

Ligands **AE-DO3A**[24] and **DMAE-DO3A**[22] were synthesized according to literature procedures. The preparation of ligands **MAE-DO3A** and **MEM-AE-DO3A** starts from *N*-methylethanolamine (Scheme 2). The latter is N-alkylated with benzyl bromide to give the tertiary ethanolamine **1**, converted into the mesylate **2** by treatment with methanesulfonyl chloride and triethylamine. Compound **2** was directly used for the alkylation of the secondary amine group of DO3A tri-*tert*-butyl ester[25] (**3**, DO3A(tBu)$_3$), operating in acetonitrile in the presence of finely powdered potassium carbonate and leading to the intermediate **4**.

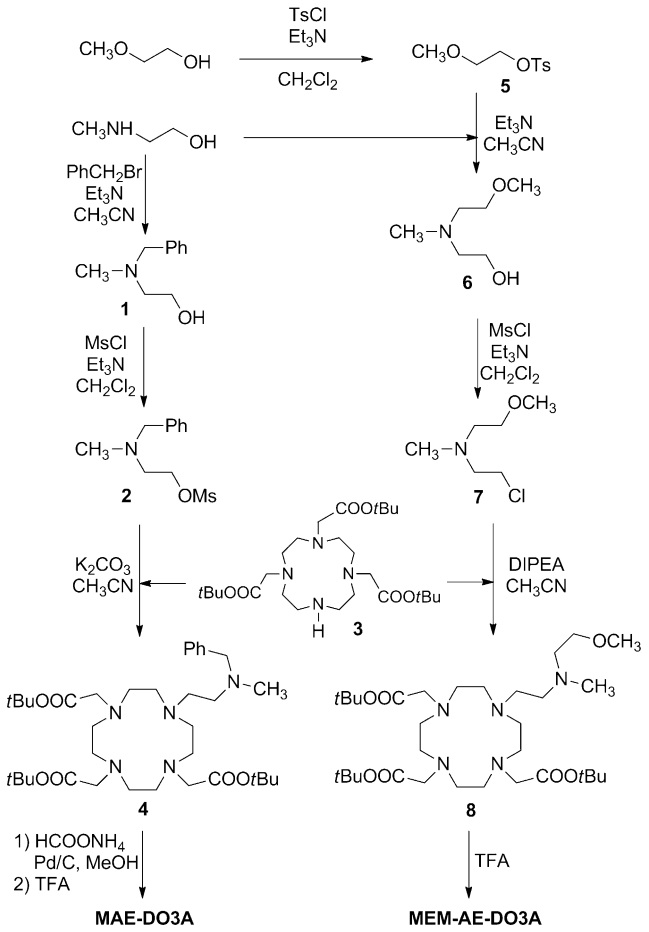

Scheme 2. Preparation of **MAE-DO3A** and **MEM-AE-DO3A**.

Removal of the benzyl group on the distal nitrogen atom was accomplished through catalytic transfer hydrogenation

($HCOONH_4$, Pd/C, MeOH heated at reflux) and the product was treated with trifluoroacetic acid (TFA) directly after the isolation from the hydrogenation step, giving the desired ligand **MAE-DO3A**.

In parallel, *N*-methylethanolamine was N-alkylated with tosylate **5**, which was easily obtained by treatment of 2-methoxyethanol with *p*-toluenesulfonyl chloride in the presence of triethylamine. Attempted mesylation of the alcoholic group of **6** with $MsCl/Et_3N$ resulted in complete conversion to the β-chloroamine **7**, likely by displacement of the first formed mesylate by the chloride anion with the anchimeric assistance of the oxygen atom of the remote methoxy group, suitably placed to form a six-membered oxonium intermediate. Nevertheless, the alkylating nature of **7** was exploited to introduce the desired structural residue on the macrocyclic ring of DO3A by treatment with DO3A(tBu)$_3$ (**3**), leading to the protected ligand **8**. Final removal of the *tert*-butyl groups from the esters yielded the ligand **MEM-AE-DO3A**.

pH dependence

The pH dependence of the relaxivity (r_{1p}) of Gd^{III} complexes of this class of DO3A-like ligands was measured to assess the viability of these complexes as responsive pH agents. Since an important issue to this end is the extent of the variation of r_{1p} (Δr_{1p}) in a clinically relevant pH range (6–8), the possibility to modulate the basicity and the steric hindrance of the pendant amino groups in this series of Gd^{III} complexes is an important feature that can give rise to interesting results. In fact, the presence of the amine leads to a protonation equilibrium that can influence the coordination cage of the Gd^{III} complex and thus its hydration state. As shown previously for Gd-**AE-DO3A** and Gd-**DMAE-DO3A**, the Gd^{III} complexes reported herein exhibit pH-dependent relaxivity due to a change in the hydration state associated with the reversible on/off ligation of the amine nitrogen donor. The pH range and the degree of variation of r_{1p} vary markedly in the series of complexes passing from Gd-**AE-DO3A**, which bears a pendant arm containing a primary amine, to Gd-**DMAE-DO3A** and Gd-**MEM-AE-DO3A**, in which tertiary amino groups are present. The pK_{aH} of the amino functionalities can be estimated by fitting the relative sigmoidal curves, characteristic of a typical two-state equilibrium process. The relaxivity variation as a function of pH is reported in Figure 1. The extimated pK_{aH} range from 5.95 for Gd-**AE-DO3A** to 7.82 for Gd-**DMAE-DO3A**, reflecting the different basicity of the substituted amino groups. Since for MRI pH-responsive applications the variation of r_{1p} has to occur around the physiological pH (between 6 and 7.4), the pK_{aH} of 6.96 for Gd-**MEM-AE-DO3A** is the most appropriate.

A preliminary analysis of the activity of these probes in Seronorm was performed to obtain an indication of the applicability of this class of Gd^{III} complexes as pH-sensitive probes in vivo, in which it is recognized that a number of endogenous anions can displace coordinated water molecules of Gd-DO3A-like complexes masking the effect that is active in H_2O.[26] Thus, the measure of the pH dependence of r_{1p} for Gd-**MEM-AE-DO3A** in Seronorm showed that pK_{aH} = 7.7 is slightly shifted to basic pH and the Δr_1 is reduced (Figure S1 in the Supporting Information).

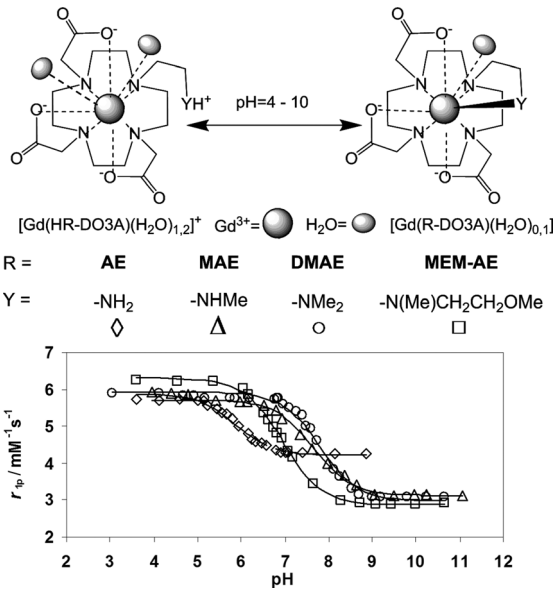

Figure 1. Relaxivity (r_{1p}) variation as a function of pH for the Gd-aminoethyl-**DO3A** complexes (◇ = **Gd-AE-DO3A**, □ = Gd-**MEM-AE-DO3A**, △ = **Gd-MAE-DO3A**, ○ = **Gd-DMAE-DO3A**).

Concerning the relaxivity values, for all the complexes r_{1p} at acidic pH is roughly similar, ranging from 5.7 to 6.2 $mM^{-1}s^{-1}$ (20 MHz and 298 K). By increasing the pH, the relaxivity steadily decreases proportionally to the decrease in the hydration state q reaching a limiting value of 4.1 $mM^{-1}s^{-1}$ for Gd-**AE-DO3A** and about 3 $mM^{-1}s^{-1}$ at pH 9 for the other Gd^{III} complexes. The Δr_{1p} observed with these Gd^{III} complexes ranges from 1.6 $mM^{-1}s^{-1}$ in case of Gd-**AE-DO3A** to 3.4 $mM^{-1}s^{-1}$ for Gd-**MEM-AE-DO3A**. These r_{1p} variations are lower than those observed for Gd-**DO3A**-sulfonamidoethyl systems ($\Delta r_{1p} \approx 6\ mM^{-1}s^{-1}$), in which there is a more evident switch from $q = 2$ to $q = 0$ hydration states of the Gd^{III} complex as a consequence of the on/off ligation switch. In fact, for low-molecular-weight monohydrated Gd^{III}-chelates ($q = 1$), as the clinically used MRI contrast agents, the relaxivity assumes a value of about 4–5 $mM^{-1}s^{-1}$ measured at 20 MHz and 298 K. Among our complexes, the r_{1p} value of 4.1 $mM^{-1}s^{-1}$ for Gd-**AE-DO3A** at pH > 7.5 approximately indicates a $q = 1$ Gd^{III} complex, whereas for the other complexes the relaxivity-limiting values at acid and basic pH are not easily attributable to Gd^{III} complexes with a distinct hydration state. For this reason, the hydration number of the complexes at both acidic and basic pH was independently determined by luminescence lifetime measurements on analogue Eu^{III} complexes following a well-established method.[27] The emission lifetimes of the Eu($^5D_0$) excited levels were measured in D_2O and H_2O solutions of the complexes, and were used to calculate the number of coordinated water molecules q (Table 1). The luminescence lifetimes determined for all four Eu complexes at acidic pH with the protonated pendant amino groups lead to a fractional value of hydration number of about 1.3, revealing the possible presence of an equilibrium in solution involving a nine-coordinated species

Table 1. Lifetimes of the Eu($^5D_0$) excited states in Eu-**AE-DO3A**, Eu-**MAE-DO3A**, Eu-**DMAE-DO3A**, Eu-**MEM-AE-DO3A** complexes and hydration number (q).

Complex	Acidic pH[a]			Basic pH[a]		
	τ_{H_2O} [ms]	τ_{D_2O} [ms]	q[b]	τ_{H_2O} [ms]	τ_{D_2O} [ms]	q[b]
Eu-**AE-DO3A**	0.48	1.47	1.4	0.57	1.41	1.0
Eu-**MAE-DO3A**	0.48	1.37	1.3	0.65	1.03	0.4
Eu-**DMEA-DO3A**	0.50	1.54	1.3	0.80	1.61	0.4
Eu-**MEM-AE-DO3A**	0.49	1.35	1.3	0.71	1.30	0.4

[a] The pH/pD values used for Eu-**AE-DO3A** are 4.5 and 7.5; for all the other complexes pH/pD = 5 and 9 were used; [b] $q^{Eu} = 1.2(1/\tau_{H_2O} - 1/\tau_{D_2O} - 0.25)$ as reported in ref. [27].

with $q = 2$ and an eight-coordinated species with $q = 1$. This may be due to the formation of hydrogen bonds between the protonated amine and the inner-sphere water molecules that hinders the coordination of a second water molecule to the metal centre. The results obtained at basic pH when the free amino group can bind the lanthanide ion are different for Eu-**AE-DO3A** with respect to the other Eu^{III} complexes. In fact, whereas for Eu-**AE-DO3A** the data are consistent with the presence of one inner-sphere water molecule, for the other Eu^{III} complexes the hydration number results again fractional (q = 0.4), which might be attributed to an equilibrium between two differently hydrated species ($q = 0$ and $q = 1$) with eight- and nine-coordination geometries.

^{1}H NMR spectroscopic study on Eu^{III} complexes

To get more insight, the structural and dynamic properties of Eu-**AE-DO3A**, Eu-**MAE-DO3A** and Eu-**DMAE-DO3A** were investigated by using ^{1}H NMR spectroscopy at pH 10 and at low temperatures (270, 280 and 290 K). Basic pH was chosen as the coordination of the amino group in the Eu^{III} complexes would result in a more rigid structure with C_1 symmetry. On the other hand, the solution structure of the protonated Eu-H**AE-DO3A**, Eu-H**MAE-DO3A** and Eu-H**DMAE-DO3A** complexes likely resembles that of the corresponding Ln-DO3A complexes characterized by a fast fluxional motion even at low temperature.

The solution structure of the Ln^{III} complexes with this class of DO3A-like ligands is expected to be similar to that of the corresponding Ln-DOTA (DOTA = 1,4,7,10-tetraazacyclododecane-1,4,7,10-tetraacetic acid) complexes, which was analysed in the solid state by using X-ray diffraction and in solution by ^{1}H- and ^{13}C NMR spectroscopy.[28–31] The detailed structural characterization of Ln-DOTA complexes indicates that, because of their rigid structure, the helicity of the four identically oriented ethylene groups of the macrocycle results in two conformation geometries (λλλλ or δδδδ) of the Ln-DOTA complexes. Similarly, the acetate groups can be oriented with two different helicities labelled by Λ and Δ. Considering all possible conformers, two enantiomer pairs (Λ(λλλλ) and Δ(δδδδ); Δ(λλλλ) and Λ(δδδδ)) may be formed in solution. Therefore, ^{1}H- and ^{13}C NMR studies on several Ln-DOTA complexes revealed the presence of two sets of signals associated to two different coordination isomers characterized with the same conformation of the macrocyclic ring but with different orientation of the side arms (i.e., capped square-antiprismatic geometry, SAP, and capped twisted square antiprismatic geometry, TSAP).[28,31] In solution, the conformation isomers of Ln-DOTA complexes can give rise to exchange processes through macrocyclic ring inversion ((λλλλ)⇌(δδδδ)) and acetate arms rotation (Λ⇌Δ) in the temperature range of 0–100 °C.[28,31] Detailed NMR structural studies on Ln-DOTA-like complexes indicated that the relative population of the SAP and TSAP isomers is affected by the size of the Ln^{III} ions.[28,31]

The substitution of one acetic arm with aminoethyl moieties reduces the symmetry removing the proton equivalence and likely decreases the rigidity of the coordination cage due to the higher flexibility of the ethylene group. The ^{1}H NMR spectra of Eu-**AE-DO3A** and Eu-**MAE-DO3A** at 270, 280 and 290 K (Figures S2 and S3, the Supporting Information) show one set of signals that can be interpreted by the predominance of one isomer in solution at pH 10. In fact, the chemical shifts of the four axial ring protons (H_a: $\delta = 24.7$, 13.3, 13.3, and 12.1 ppm for Eu-**AE-DO3A** and H_a: $\delta = 33.9$, 32.8, 31.0, and 23.1 ppm for Eu-**MAE-DO3A**), are respectively similar to those of the TSAP and SAP isomers of Eu-DOTA,[28] indicating the prevalence of different isomers for the two complexes. On the other hand, the ^{1}H NMR spectra of Eu-**DMAE-DO3A** (Figure S4, the Supporting Information) contain two sets of well-separated signals indicating the presence of both SAP and TSAP isomers. The chemical shifts of the axial ring protons of the major H_a: δ = 38.5, 36.4, 31.7, and 28.0 ppm and minor H'_a: $\delta = 19.9$, 19.1, 18.1, and 16.8 ppm isomers of Eu-**DMAE-DO3A** are similar to those of the SAP and TSAP isomers of Eu-DOTA, respectively. By comparing the integral of the two set of signals of axial ring-protons, the ratio between the SAP and TSAP isomers for Eu-**DMAE-DO3A** under these conditions can be estimated as about 68:32. In conclusion, the fractional hydration number can be explained by a mixture of $q = 0$ and $q = 1$ isomers with a different coordination number. However, an alternative interpretation could be given by the presence of $q = 1$ complexes with a longer Ln–water bond as reported earlier.[32]

Relaxometric properties

Since the four Gd^{III} complexes discussed in this work have relaxivities that depend on pH with significant variation of r_{1p} from basic to acidic pH, the relaxometric properties were independently studied in detail in the acidic range (pH 4.5–5) and in the basic range (pH 8–9.5). The value of r_{1p} of a Gd^{III} complex depends on the magnetic field strength, temperature, and on several important structural and dynamic molecular parameters of the metal complex that describe the magnetic interaction between the solvent nuclei and Gd^{III}.[6] The measurement of the longitudinal relaxation rates of the water proton over a wide range of magnetic fields is the best way to obtain the set of parameters governing the relaxivity. Thus, r_{1p} as a function of proton Larmor frequency (nuclear magnetic resonance dispersion, NMRD) was measured for all Gd^{III} complexes at both acidic and basic pH at 298 and 310 K over the range

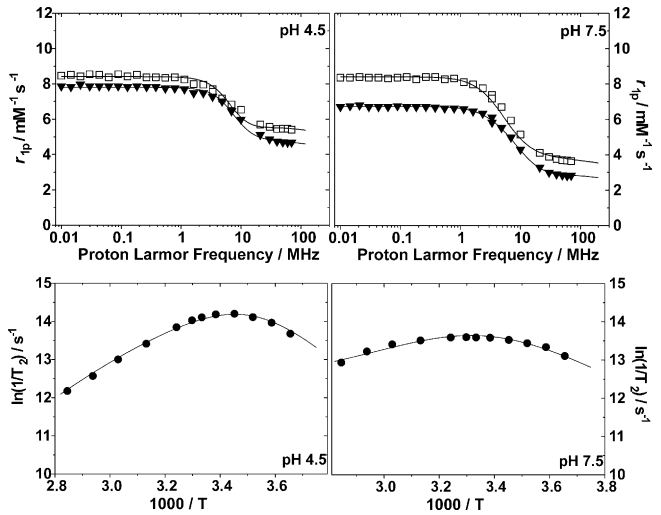

Figure 2. Top: $1/T_1$ ^{1}H NMRD relaxation data for Gd-**AE**-**DO3A** at pH 4.5 (left) and 7.5 (right), 298 K (□) and 310 K (▼). Bottom: variable-temperature ^{17}O reduced transverse relaxation rates at 11.7 T and at pH 4.5 (left) and 7.5 (right) for a 13.3 mM solution of Gd-**AE**-**DO3A**. The solid lines represent the best results of the fitting to the experimental points (Table 2).

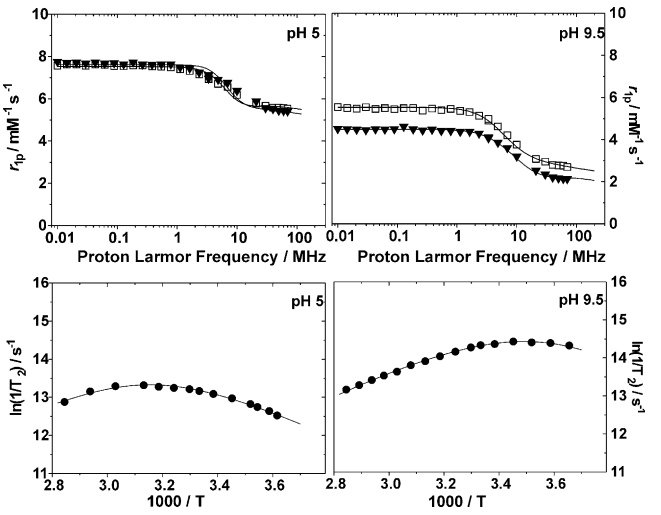

Figure 4. Top: $1/T_1$ ^{1}H NMRD relaxation data for Gd-**DMAE**-**DO3A** at pH 5 (left) and 9.5 (right), 298 K (□) and 310 K (▼). Bottom: variable-temperature ^{17}O reduced transverse relaxation rates at 11.7 T and at pH 5 (left) and 9.5 (right) for a 17.1 mM solution of Gd-**DMAE**-**DO3A**. The solid lines represent the best results of the fitting to the experimental points (Table 2).

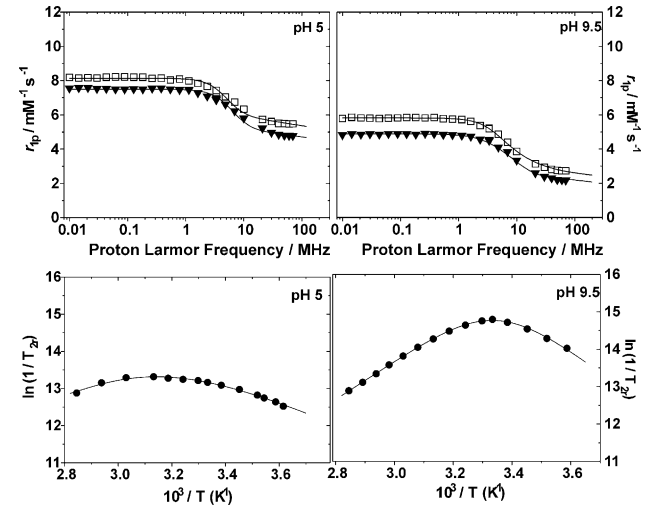

Figure 3. Top: $1/T_1$ ^{1}H NMRD relaxation data for Gd-**MAE**-**DO3A** at pH 5 (left) and 9.5 (right), 298 K (□) and 310 K (▼). Bottom: variable-temperature ^{17}O reduced transverse relaxation rates at 11.7 T and at pH 5 (left) and 9.5 (right) for a 12.8 mM solution of Gd-**MAE**-**DO3A**. The solid lines represent the best results of the fitting to the experimental points (Table 2).

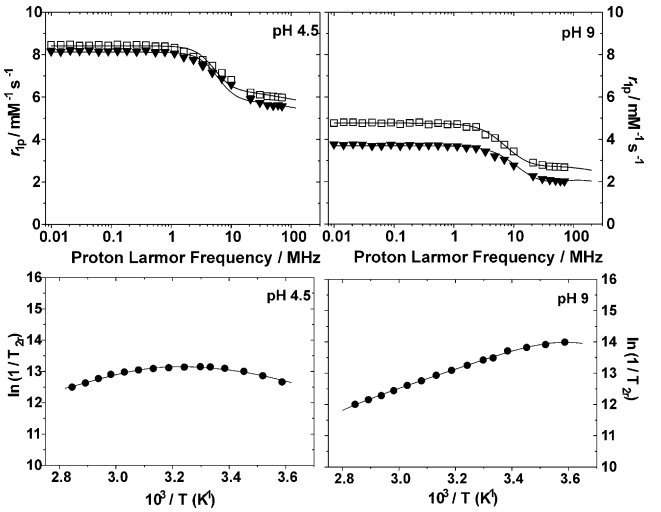

Figure 5. Top: $1/T_1$ ^{1}H NMRD relaxation data for Gd-**MEM**-**AE**-**DO3A** at pH 4.5 (left) and 9 (right), 298 K (□) and 310 K (▼). Bottom: variable-temperature ^{17}O reduced transverse relaxation rates at 11.7 T and at pH 4.5 (left) and 9 (right) for a 25.2 mM solution of Gd-**MEM**-**AE**-**DO3A**. The solid lines represent the best results of the fitting to the experimental points (Table 2).

0.01–70 MHz corresponding to magnetic field strengths varying between 2.34×10^{-4} and 1.64 T (Figure 2, Figure 3, Figure 4 and Figure 5).

To obtain more accurate information on the kinetics of the water exchange, the temperature dependence of the ^{17}O NMR transverse relaxation rate, R_2 was also measured for all Gd complexes at 11.7 T on 13–25 mM solutions of the complexes at pH 4.5–5 and pH 8–9.5.

NMRD and ^{17}O NMR spectroscopic data were analysed according to the established theory of paramagnetic relaxation expressed with the Solomon–Bloembergen–Morgan (SBM)[33] and Freed's[34] equations for the inner- and outer-sphere proton relaxation mechanisms, respectively, and with the Swift–Connick theory for ^{17}O relaxation.[35] Some parameters were fixed to reasonable values, which are well-accepted as constant for this class of complexes: 1) the distance of closest approach of the outer-sphere water protons ($a=4.0$ Å); 2) the relative diffusion coefficient of solute and solvent ($^{298}D=2.24\times10^{-5}$ cm^2 s^{-1}); 3) the metal-bound water proton distance ($r_{GdH}=3.1$ Å); 4) the Gd-^{17}O scalar coupling constant ($A/\hbar=-3.5$ rad s^{-1}). The number of coordinated water molecules q was also set to the value determined by luminescence meas-

Table 2. Selected parameters obtained from the analysis of the $1/T_1$ NMRD profiles (298 K) and ^{17}O NMR (11.7 T) data for Gd-**AE-DO3A**, Gd-**MAE-DO3A**, Gd-**DMAE-DO3A** and Gd-**MEM-AE-DO3A** and related complexes (Gd-**DO3A**[36] and Gd-**DOTAMA**-En[37]).[a]

	pH	q	τ_R [ps]	k_{ex} [$\times 10^6$ s^{-1}]	ΔH_M [kJ mol^{-1}]	Δ^2 [10^{19} s^{-2}]	τ_V [ps]
Gd-**AE-DO3A**	7.5	1	64±2	1.8±0.3	27.4±0.2	3.1±0.3	14±1
	4.5	1.4	84±2	8.3±0.2	52.0±0.6	6.2±0.5	20±2
Gd-**MAE-DO3A**	9.5	0.4	66±2	4.9±0.1	45.8±0.3	1.6±0.4	34±2
	5.0	1.3	115±2	0.65±0.05	22.3±0.6	3.4±0.2	28±1
Gd-**DMAE-DO3A**	9.5	0.4	69±4	8.1±0.1	29.6±0.3	3.5±0.5	19±2
	5.0	1.3	107±2	0.72±0.05	24.0±0.7	5.9±0.4	22±1
Gd-**MEM-AE-DO3A**	9.5	0.4	72±4	13.4±0.5	46.0±0.7	8.2±0.5	13±1
	5.0	1.3	120±2	0.68±0.01	20.1±0.5	3.7±0.2	28±1
Gd-**DOTAMA**-En	7.4	1	79	1.1	34	3.8	11
Gd-**DO3A**	7.4	1.8	66	6.2	44	4.6	14

[a] For the parameters $r_{Gd\text{-}H}$, a, ^{298}D and $A/\hbar$ the values of 3.1, 4.0 Å, 2.25×10^{-5} cm^2 s^{-1}, -3.5 rad s^{-1} were used, respectively. DOTAMA-En = DOTA monoamide-ethylenediamine

urements on the corresponding Eu^{III} complex. The best-fit parameters are listed in Table 2 and compared with those of Gd-**DO3A**[36] for data obtained at acidic pH and of a representative neutral Gd-DOTA-monoamide complex,[37] which resembles more closely the coordination cage of our Gd^{III} complexes at basic pH when the amines are bound to the metal centre. The NMRD profiles of all Gd^{III} complexes at both acidic and basic pH are characterized by a simple shape featuring a plateau at low fields, a single dispersion centred around 4–8 MHz and another plateau in the high-field region (>20 MHz), quite typical of rapidly tumbling complexes. Fitting the ^1H NMRD data allowed the confirmation of hydration and assessment of rotational motion of the Gd^{III} complexes in solution. Rotational correlation times (τ_R) of the Gd^{III} complexes at basic pH were well in agreement with those of other low molecular weight Gd^{III} chelates increasing with increasing the molecular weight within the series, from Gd-**AE-DO3A**, which contains a primary amine, to Gd-**MAE-DO3A**, which bears a secondary dialkylamine, to Gd-**DMAE-DO3A** and Gd-**MEM-AE-DO3A**, carrying tertiary amines. On the contrary, slightly higher τ_R values were obtained for the protonated species at acidic pH. This could be due either to a larger solvation sphere around the protonated amine, which causes an increase of the hydrodynamic radius of the species in solution, or to the moving away from the Gd^{III} centre of the aminoethyl substituent upon its protonation, which results in a less compact molecule with higher molecular volume. The analysis of both ^1H NMRD and ^{17}O NMR data yielded electronic spin parameters (Δ^2, τ_V) in good agreement with literature values. The most interesting finding is related to a significant variation in water exchange regime observed within the series and upon pH modulation. A qualitative indication can be also drawn from the temperature dependence of the relaxivity at both acidic and basic pH that was measured for all complexes to further confirm the presence of fast or slow water exchange regimes (Figure 6). In fact, a steep exponential decay with temperature is indication of fast exchange regime, in which a low value of τ_M ($k_{ex}=1/\tau_M$) does not limit ^1H inner-sphere relaxivity, whereas a shallower variation with temperature indicates higher τ_M values that can limit ^1H inner-sphere $1/T_1$ as exemplified by Equation (1):[7]

$$\frac{1}{T_1^{IS}} \propto \frac{1}{\tau_M + T_{1M}} \quad (1)$$

A more accurate estimate of this effect was assessed by ^{17}O NMR experimental data, especially at basic pH for the mono-aqua Gd-**AE-DO3A** and for the other Gd complexes present at about 40% in the $q=1$, nonacoordinate form (Figures 2–5). The trend along the series highlights that the water exchange rate is slower (1.8×10^6 s^{-1}) for Gd-**AE-DO3A**, when the primary amine coordinates the metal centre and it increases moving to the coordination of a secondary amine with Gd-**MAE-DO3A** (4.9×10^6 s^{-1}) and of a tertiary amine with Gd-**DMAE-DO3A** (8.1×10^6 s^{-1}).

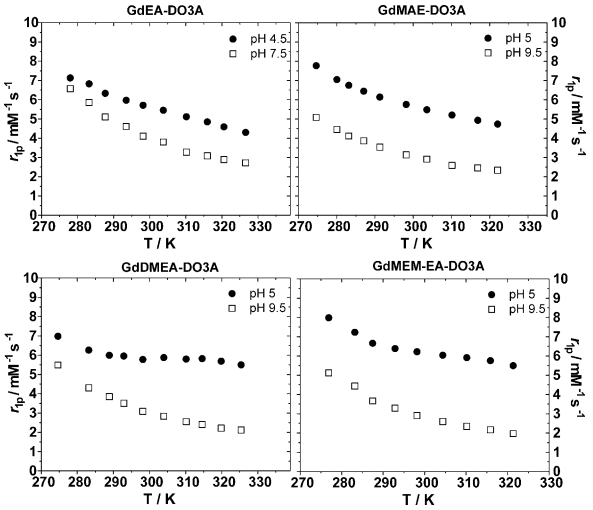

Figure 6. Temperature dependence of r_{1p} for Gd-**AE-DO3A**, Gd-**MAE-DO3A**, Gd-**DMAE-DO3A**, and Gd-**MEM-AE-DO3A** (pH 7.0, 20 MHz).

A further increase was observed for Gd-**MEM-AE-DO3A** (13.4×10^6 s^{-1}). This behaviour can be attributed both to an increase in basicity of the amine, as already shown by the differences in pK_{aH} reported previously, and to the steric hindrance of the amino group. In fact, the coordination between the amine and the Gd^{III} ion causes a destabilisation of the Gd^{III}–O(water) bond as expected on the basis of the stereoelectronic effect of the alkyl groups on the pendant amine. A similar trend was reported in the case of the Gd^{III} complexes with DO3AM (1,4,7,10-tetraazacyclododecan-1,4,7-triacetamide) and Me-DO3AM (10-methyl-1,4,7,10-tetraazacyclododecan-1,4,7-triacetamide), in which a secondary and a tertiary amine, respectively, coordinate the metal centre and induce a 2.5-fold increase in the water-exchange rate.[38] In the case of Gd-**MEM-AE-DO3A**, the bulkier methoxyethyl group may be responsible for a further increase of k_{ex}. It should be noted that only the $q=1$ fraction of the Gd^{III} complexes at basic pH was considered in the fitting of the ^{17}O NMR data, whereas at acidic pH the presence of

a mixture of $q=1$ and $q=2$ allowed us to obtain average values of parameters of the two states. In general, the analysis of the ^{17}O data of the Gd^{III} complexes at acidic pH allows us to emphasize a particularly low water-exchange rate for Gd-**MAE-DO3A**, Gd-**DMAE-DO3A**, and Gd-**MEM-AE-DO3A** confirmed also by the shape of the temperature-dependence curve (Figure 6), which resembles closely that of the triply charged Gd-DOTAM (1,4,7,10-tetraazacyclododecan-1,4,7,10-tetraacetamide) complexes.[39] This result suggests a possible hydrogen-bonding interaction between the coordinated water molecule and the protonated amine, either directly or involving an intermediate water molecule. A similar behaviour was observed for ternary complexes between Gd-DO3AM and fluoride or phosphate anions.[12] On the other hand, a possible explanation for the fast water-exchange rate determined at acidic pH for Gd-**AE-DO3A** is that the protonated complex is present in a coordination isomer with a fast k_{ex} influencing the average τ_M value dramatically. In fact, it is well-known that the two TSAP and SAP isomers of Gd-DOTA-like derivatives are associated with markedly different inner-sphere water-exchange dynamics.[40]

Solution equilibrium studies

The assessment of the thermodynamic stability of Ln^{III} complexes with this class of aminoethyl-DO3A ligands is of particular interest because they behave as heptadentate ligands in acidic conditions and octadentate at higher pH values when the pendant amine coordinates the metal ion. These two coordination environments are characteristic of DO3A- and DOTA-like ligands, respectively. In this regard, the stability constants ($\log K_{LnL}$) of Ln-DOTA-like complexes are 3–4 orders of magnitude higher than those of the corresponding Ln-DO3A-like complexes. The solution thermodynamic and kinetic study was carried out only on **AE-DO3A** and **DMAE-DO3A** ligands because they represent the two extremes of the series of this class of DO3A-like ligands having primary to tertiary amines on the pendant arms.

Protonation equilibria: The protonation constants of H_3**AE-DO3A** and H_3**DMAE-DO3A**, as defined by Equation (2), were determined by pH potentiometry. The $\log K_i^H$ values obtained are listed and compared with those of H_4**DOTA** and H_3**DO3A** in Table 3 (standard deviations are shown in parentheses).

Table 3. Protonation constants of H_3**AE-DO3A**, H_3**DMAE-DO3A**, H_3**DO3A**, and H_4DOTA (0.1 M KCl, 298 K).

	H_3**AE-DO3A**	H_3**DMAE-DO3A**	H_3**DO3A**[a]	H_4**DOTA**[a]
$\log K_1^H$	12.49 (2)	11.92 (1)	11.99	11.41
$\log K_2^H$	10.38 (2)	9.84 (2)	9.51	9.83
$\log K_3^H$	8.80 (2)	8.72 (2)	4.30	4.38
$\log K_4^H$	4.03 (2)	4.25 (2)	3.63	4.63
$\log K_5^H$	1.70 (3)	1.93 (2)	1.84	1.92
$\log K_6^H$	–	–	–	1.58
$\Sigma\log K_i^H$	37.40	36.83	31.26	33.75

[a] Ref. [42].

$$K_i^H = \frac{[H_iL]}{[H_{i-1}L][H^+]} \quad (2)$$

in which $i=1, 2\ldots6$. The protonation scheme of DOTA-like ligands was well characterized by both spectroscopic and potentiometric methods.[41–43] Thus, the first and second protonation processes occur at two diagonal ring nitrogen atoms, whereas the third and fourth protonations take place at the carboxylate groups attached to the non-protonated ring nitrogen atoms due to larger charge separation, H-bond network and electrostatic repulsion between the protonated donor atoms.[41,43]

A comparison of protonation constants of **AE-DO3A** and **DMAE-DO3A** with those of DOTA and DO3A, indicates that $\log K_1^H$ and $\log K_2^H$ of **AE-DO3A** are the highest (Table 3), whereas $\log K_4^H$ and $\log K_5^H$ are comparable with those of DOTA and DO3A. The higher first and second protonation constants of **AE-DO3A** might be explained by the formation of a H-bond between the protonated ring nitrogen and the primary amino group stronger than that formed between the protonated ring nitrogen and acetate groups in DOTA.[41] On the other hand, in case of **DMAE-DO3A**, $\log K_1^H$ and $\log K_2^H$ are lower than those of **AE-DO3A**, possibly due to a weaker H-bond between the protonated ring nitrogen atoms and the dimethylamino group of the side chain for its steric hindrance. Although the pK_a of simple ethyl- and dimethylethylamines are 10.7 and 10.4, respectively,[44] the third protonation of **AE-DO3A** and **DMAE-DO3A** should take place at the nitrogen atom of the pendant amino group. These values lower than the free isolated amines can be explained by the electrostatic repulsion between the first, second and the entering third proton, and by the presence of a H-bond between the protonated ring-nitrogen atoms and the amino group of the pendant arm. Finally, $\log K_4^H$ and $\log K_5^H$ correspond to the protonation of two carboxylate groups. The $\Sigma\log K_i^H$ values (Table 3) indicate that the total basicity of **AE-DO3A** and **DMAE-DO3A** is higher than that of DOTA and DO3A because of the relatively high protonation constant of the pendant amine nitrogen atom. Since the protonation of the different donor atoms does not take place independently, the total basicity of ligands indirectly affects the stability of its metal complexes. Therefore, the thermodynamic stability of **AE-DO3A** and **DMAE-DO3A** complexes, in the case of the coordination of the pendant amino group, should be comparable or even higher than those of DOTA and DO3A complexes. The coordination of this amine to the metal ion may play an important role in the complexation, since it increases the denticity of the ligand from heptadentate to octadentate. On the other hand, it is well-known that non-ionic donor atoms are more weakly bound to Ln^{III} ions than ionic donor atoms, so the equilibrium study of the metal complexes of **AE-DO3A** and **DMAE-DO3A** would give new insights into the effects on the complex stability of the interaction between the non-protonated amino group and the metal ions.

Complexation properties: The stability and protonation constants of **AE-DO3A** and **DMAE-DO3A** complexes with several

Table 4. Stability ($\log K_{ML}$) and protonation ($\log K_{MH_iL}$) constants of the Ca^{II}, Zn^{II}, Cu^{II}, and Ln^{III} complexes of the **AE-DO3A**, **DMAE-DO3A**, **DO3A** and **DOTA** ligands (0.1 M KCl, 298 K).

	H_3**AE-DO3A**	H_3**DMAE-DO3A**	H_3**DO3A**[a]	H_4**DOTA**[a]		H_3**AE-DO3A**	H_3**DMAE-DO3A**	H_3**DO3A**[a]	H_4**DOTA**[a]
CaL	14.00 (5)	12.68 (1)	12.57	16.11	LaHL	6.64 (3)	8.21 (3)	–	–
CaHL	7.44 (5)	8.72 (1)	4.60	3.67	LaH_2L			*6.27	*7.61 (2)
CaH_2L	–	5.20 (3)	–	–	LaH_3L	*4.91 (1)	*5.58 (3)		
ZnL	21.45 (6)	20.09 (5)	21.57	20.21	GdL	22.40 (6)	20.56 (1)	21.56	24.7[b]
ZnHL	7.48 (3)	8.75 (3)	3.47	4.12	GdHL	5.91 (7)	7.98 (4)	–	–
ZnH_2L	4.10 (1)	3.92 (2)	2.07	3.49	GdH_2L			*5.93	*7.25 (2)
ZnH_3L	2.14 (5)	2.63 (2)	–	2.56	GdH_3L	*4.89 (5)	*6.01 (4)		
CuL[c]	25.36 (4)	24.80 (7)	25.89	24.83	LuL	22.09 (4)	20.63 (8)	21.44	25.4[b]
CuHL	7.35 (3)	8.69 (3)	3.65	4.12	LuHL	6.53 (7)	7.73 (3)	–	–
CuH_2L	3.67 (2)	3.79 (2)	1.81	3.57	LuH_2L			*5.69	*7.46 (2)
CuH_3L	1.41 (8)	1.47 (2)	–	0.87	LuH_3L	*4.44 (4)	*5.71 (3)		
LaL	20.23 (3)	18.50 (9)	18.63	21.7[b]					

[a] Ref. [42]; [b] ref. [48]; [c] measured by spectrophotometry (298 K). [*] = Stability constants of the protonated *Ln(H_iL) intermediate $*K_{Ln(H_iL)} = [Ln(H_iL)]/[Ln^{3+}][H_iL]$, where $i = 3$ for AE-DO3A and DMAE-DO3A; $i = 2$ for DO3A and DOTA.

metal ions were investigated by pH-potentiometric, UV/Vis spectrophotometric and ^{1}H NMR relaxometric methods (298 K, 0.1 M KCl; Table 4). The formation of the protonated *Ln(H_iL) intermediates were also considered in our equilibrium studies as already reported for Ln-DOTA complexes.[45–47] The experimental details and the equations used for the evaluation of the equilibrium data are summarized in the Supporting Information.

The stability constants of Ca^{II}- and Ln^{III} complexes with **AE-DO3A** are generally about 1–2 orders of magnitude higher than those of the corresponding **DMAE-DO3A** and DO3A complexes. The $\log K_{ML}$ of Zn^{II}- and Cu^{II} complexes of **AE-DO3A** are similar to those observed for DO3A and higher than those with **DMAE-DO3A** and DOTA probably due to its higher first and second protonation constants. The similar stability of Ca^{II}- and Ln^{III} complexes with **DMAE-DO3A** and DO3A indicates that the pendant dimethylamino group does not affect significantly the $\log K_{ML}$ values likely due to its steric hindrance in the coordination of the metal ions.

The stability constants of Ln-**AE-DO3A** and Ln-**DMAE-DO3A** complexes increase from La^{III} to Gd^{III}, then they remain practically constant for the lanthanides with lower size (Table 4) as already found for Ln-DO3A and Ln-DOTA complexes.[7] This result clearly indicates that the size match between the lanthanide ions and the coordination cage determined by the ring-nitrogen atoms, the acetate oxygen atoms, and the amino N-atom is optimal for Gd^{III}. The protonation constants of the amino group of Ln-**AE-DO3A** and Ln-**DMAE-DO3A** complexes depends on the nature of the Ln^{III} ion (Table 4) as also observed for Ln-**DO3A-SA** complexes.[42] In particular, $\log K_{LnHL}$ for Ln-**AE-DO3A** are in the range 5.9–6.7, 2–3 orders of magnitude lower than the correspondent protonation constant of the free ligand ($\log K_3^H$). These findings indicate that the interaction between the Ln^{III} ions and the free amine is strong and can be responsible for the higher $\log K_{LnL}$ of Ln-**AE-DO3A** with respect to Ln-DO3A. On the other hand, $\log K_{LnHL}$ of Ln-**DMAE-DO3A** are in the range of 7.7–8.2, decreasing from La^{III} to Lu^{III}, and closely similar to $\log K_3^H$ of the free ligand. Thus, it can be assumed that in this case the interaction between dimethylamino group and Ln^{III} ions is relatively weak.

It must be highlighted that the protonation and/or stability constants of Gd^{III}-, Ce^{III}- and Cu^{II} complexes with **AE-DO3A** and **DMAE-DO3A** were independently determined by using other experimental methods and very similar $\log K$ values were obtained, thus confirming the accuracy of the measured data (see the Supporting Information for details). In particular, $\log K_{GdL} = 22.36(8)$ and $\log K_{GdHL} = 5.95(2)$ (for L = **AE-DO3A**) and $\log K_{GdL} = 20.72(7)$ and $\log K_{GdHL} = 7.82(3)$ (for L = **DMAE-DO3A**) were determined by measuring the relaxivities of equilibrium solutions of Gd^{III}/**AE-DO3A** and Gd^{III}/**DMAE-DO3A** systems in separate samples (out-of-cell method) in the pH range 2.8–4.0 (see the Supporting Information, Figure S7, 20 MHz, 0.1 M KCl, 298 K). Moreover, protonation constants of Ce-**AE-DO3A** ($\log K_{CeHL} = 6.33(3)$) and Ce-**DMAE-DO3A** ($\log K_{CeHL} = 8.20(8)$), Cu-**AE-DO3A** ($\log K_{CuHL} = 7.64(5)$) and Cu-**DMAE-DO3A** ($\log K_{CuHL} = 8.74(6)$) were determined by measuring the UV/Vis absorption spectra at different pH values (see the Supporting Information, Figures S5, S6, S9 and S10). Additionally, the pendant amino nitrogen atom of Ca^{II}-, Zn^{II}- and Cu^{II} complexes with **AE-DO3A** and **DMAE-DO3A** can be protonated leading to $\log K_{MHL}$ values (Table 4) similar to $\log K_3^H$ of the free ligands. This finding indicates that in these complexes the pendant amines are either uncoordinated or are only weakly coordinated giving rise to a structure very similar to analogous DO3A complexes. More details on the structural behaviour of Cu-**AE-DO3A** and Cu-**DMAE-DO3A** are given in the Supporting Information in Figures S10–S12. Finally, these Ca^{II}-, Zn^{II}- and Cu^{II} complexes, similarly to those of the DOTA and DO3A, form di- and triprotonated species at lower pH values, in which one and two free carboxylate groups are protonated, respectively.

Kinetic studies

Complex formation kinetics: The complex formation reactions between **AE-DO3A** and **DMAE-DO3A** and Ln^{III} ions were found to be slow in the pH range 4–6 in which the protonated Ln-H**AE-DO3A** and Ln-H**DMAE-DO3A** species are present. It is well-established that the formation of the Ln^{III} complexes with macrocyclic ligands is generally slow;[45–47,49–53] for example, the introduction of Ln^{III} ions into the rigid and preformed coordi-

nation cage of DOTA-like ligands is slow because of the formation of the unusually stable diprotonated intermediates, *Ln-H_2DOTA, which could be detected by spectrophotometry,[45,49] ^{1}H NMR[50] and luminescence spectroscopy.[46,47] The luminescence lifetime study of the intermediate *Eu-H_2DOTA revealed that the number of H_2O molecules directly coordinated to the Eu^{III} was between four and five, suggesting the out-of-cage coordination by four carboxylates with two diagonal nitrogen atoms of the ring being protonated.[46,47,49,50] The stability constants of the intermediates were also calculated from the data obtained by kinetic,[50] direct pH-potentiometric,[45] UV/Vis[45] and luminescence spectroscopy measurements.[46,47] The first step of the complexation was shown to be the rapid formation of the diprotonated *Ln-H_2DOTA intermediate in equilibrium with a monoprotonated *Ln-HDOTA intermediate. The deprotonation of the latter, that is an OH^--assisted reaction is the rate-determining step of Ln-DOTA formation.[45–47,49,51–53]

The rates of the formation reactions of Ce^{III}- and Eu^{III} complexes with **AE-DO3A** and **DMAE-DO3A** were studied by spectrophotometry in the presence of 5–40 fold excess of Ln^{III} ions in the pH range 4.5–6.0. The plots of k_{obs} values versus [Ln^{III}] gave saturation curves, which clearly indicates the formation of reaction intermediates (see the Supporting Information, Figures S11 and S12). This phenomenon can be interpreted by the rapid formation of a triprotonated intermediate that can be deprotonated and rearranged to the final product (Ln-H**AE-DO3A** and Ln-H**DMAE-DO3A**) in a slow, rate-determining step. As already shown in the thermodynamic study section, the formation of the Ln-**AE-DO3A** and Ln-**DMAE-DO3A** complexes occurs through the formation of a triprotonated *Ln-H_3L out-of-cage complex (intermediate) in which three carboxylate groups are coordinated to the Ln^{III} ion and two diagonal ring and the amino nitrogen atoms are protonated. The rate-determining step of the formation of the Ln-H**AE-DO3A** and Ln-H**DMAE-DO3A** complexes is then the deprotonation of a ring nitrogen of the *Ln-H_2**AE-DO3A** and *Ln-H_2**DMAE-DO3A** intermediates and the rearrangement to the final product. The proposed mechanism for the formation of Ln-H**AE-DO3A** and Ln-H**DMAE-DO3A** complexes is shown in Scheme 3. The definitions and equations used for the evaluation of the kinetic data are reported in the Supporting Information.

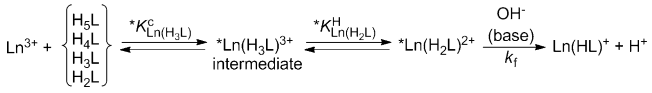

Scheme 3. The suggested pathway for the formation of Ln-H**AE-DO3A** and Ln-H**DMAE-DO3A** complexes.

In Scheme 3, $^*K^C_{Ln(H_3L)}$, $^*K^H_{Ln(H_2L)}$ and k_f are the conditional stability constants of *Ln-H**AE-DO3A** and *Ln-H**AE-DO3A**, the protonation constants of *Ln-H_2**AE-DO3A** and *Ln-H_2**DMAE-DO3A** and the rate constants characterising the deprotonation and rearrangement of the intermediates to the Ln-H**AE-DO3A** and Ln-H**DMAE-DO3A** complexes. The conditional stability constants ($^*K^C_{Ln(H_3L)}$) of *Ce-H_3L and *Eu-H_3L intermediates obtained from the kinetic data are 2.2(1) and 1.8(1) for **AE-DO3A** and 2.2(1) and 2.5(1) for **DMAE-DO3A**, respectively. These values are higher than the conditional stability constants of the diprotonated *Ln-H_2-1,7-DO2A (1,7-DO2A = 1,4,7,10-tetraazacyclododecane-1,7-diacetic acid) intermediates (*Ce-H_2-1,7-DO2A: 1.98, *Yb-H_2-1,7-DO2A: 1.60)[52] and lower than those reported for the diprotonated *Ln-H_2DO3A and *Ln-H_2DOTA intermediates (*Gd-H_2DO3A: 3.48, *Ce-H_2DOTA: 4.4, *Eu-H_2DOTA: 4.3).[45,51] The electrostatic repulsion between the Ln^{III} ion and the protonated pendant amino group may be responsible for the reduction of $^*K^C_{Ln(H_3L)}$ values for *Ln-H_3**AE-DO3A** and *Ln-H_3**DMAE-DO3A**. However, it can be assumed that the structure of *Ln-H_3**AE-DO3A** and *Ln-H_3**DMAE-DO3A**, that is, the number of the acetate arms coordinated to the Ln^{III} ion, is similar to those of *Ln-H_2DO3A intermediates.

The rate constants k_f as a function of [OH^-] obtained for the formation of the Ce^{III}- and Eu^{III} complexes of **AE-DO3A** and **DMAE-DO3A** are shown in Figure 7. These data indicate that k_f displays a second-order dependence on the OH^- concentration, expressed by Equation (3):

$$k_f = k_{OH}[OH^-] + k_{OH^2}[OH^-]^2 \quad (3)$$

This kind of rate law is quite unusual as, typically, k_f for Ln-DOTA-like complexes shows a first-order dependence on [OH^-].[45–47,49–51,53] For these systems k_{OH} and k_{OH^2} are the rate constants characterizing the OH^--assisted deprotonation and rearrangement of the out-of-cage intermediates to the final complexes. Similar second-order dependence of k_f on [OH^-] was reported for the formation of Ln^{III} complexes with DOTA-phosphonate derivatives.[54] The rate constants k_{OH} and k_{OH^2} were calculated by fitting k_f rate constants (Figure 7) to Equation (3) and are reported in Table 5 and Table 6 compared to analogous data of Ln-DOTA and Ln-DOTA-like complex formation.

The first-order dependence of k_f on [OH^-], expressed by the k_{OH} rate constants, can be interpreted by the rapid deprotona-

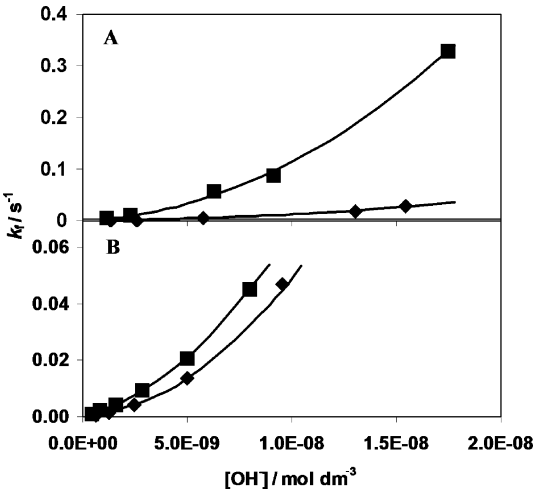

Figure 7. The k_f rate constants for the formation reactions of the a) Ln-H**AE-DO3A**, and b) Ln-H**DMAE-DO3A** complexes of Ce^{III} (◆) and Eu^{III} (■) as a function of [OH^-] (0.1 M KCl, 298 K).

Table 5. The k_{OH} [$M^{-1}s^{-1}$] of **AE-DO3A**, **DMAE-DO3A**, **DOTA**, **DO3A**, 1,7-**DO2A** and **DOA3P** complexes with Ce^{III} and Eu^{III} (0.1 M KCl, 298 K).

	Ce^{III}	Eu^{III}
AE-DO3A^{3-}	$(1.4\pm0.1)\times10^{5}$	$(1.7\pm0.2)\times10^{6}$
DMAE-DO3A^{3-}	$(6.5\pm0.1)\times10^{5}$	$(1.8\pm0.1)\times10^{6}$
DOTA^{4-} [a]	3.5×10^{6}	1.1×10^{7}
DO3A^{3-} [b]	–	2.1×10^{7} (Gd^{III})
1,7-DO2A^{2-} [c]	2.8×10^{5}	2.5×10^{5} (Yb^{III})
DOA3P^{7-} [d]	–	2.2×10^{4} (Gd^{III})

[a] Ref. [45]; [b] ref. [51]; [c] ref. [53]; [d] ref. [54]. DO3AP = 1,4,7,10-tetraazacyclododecane-4,7,10-tris(carboxymethyl)-1-methylphosphonate

Table 6. The k_{OH^2} [$M^{-2}s^{-1}$] rate constants characterizing the formation of **AE-DO3A**, **DMAE-DO3A** and **DOA3P** complexes formed with Ce^{III} and Eu^{III} (0.1 M KCl, 298 K).

	Ce^{III}	Eu^{III}
AE-DO3A^{3-}	$(1.1\pm0.1)\times10^{14}$	$(9.7\pm0.5)\times10^{14}$
DMAE-DO3A^{3-}	$(4.2\pm0.1)\times10^{14}$	$(4.8\pm0.2)\times10^{14}$
DOA3P^{7-} [a]	–	3.8×10^{11}

[a] Ref. [54].

tion of the triprotonated to the diprotonated *Ln-H_2**AE-DO3A** and *Ln-H_2**DMAE-DO3A** intermediates in the equilibrium reaction, followed by the release of the second proton in the OH^--assisted rate-determining step and a final structural rearrangement of the complex. The k_{OH} values of our systems (Table 5) are lower than those of Ln-DO3A complexes probably due to the presence of the positively charged side chain leading to lower stabilities of the formed triprotonated *Ln(H_3L) intermediates. The second-order dependence of k_f rate constants on [OH^-] can be explained by assuming the OH^--assisted deprotonation of the aminoethyl pendant arm, which can then act as a general base for the proton transfer and rearrangement of the out-of-cage intermediates to the final Ln-H**AE-DO3A** and Ln-H**AE-DO3A** complexes. The validity of general base catalysis was proved for Ln-DOTA and some Ln-DO3A-like complexes,[51,53] for which the rate-controlling step is the deprotonation of a *Ln–H_2L intermediate followed by a structural rearrangement with the Ln^{III} ion settling into the "coordination cage" formed by the ring nitrogen atoms and the carboxylate oxygen atoms of the ligand.[45–47,49,51–53] Compared with the DOTA-phosphonate system, the k_{OH^2} for Ln-H**AE-DO3A** and Ln-H**DMAE-DO3A** are three orders of magnitude higher than for Gd-DOA3P probably due to the different basicity of the pendant amino- (**AE-DO3A**: $\log K_3^H = 8.8$, **DMAE-DO3A**: $\log K_3^H = 8.7$, Table 3) and phosphonate groups (DOA3P: $\log K_3^H = 7.7$, $\log K_4^H = 6.33$, $\log K_5^H = 5.13$).[54]

Dissociation kinetics: The kinetic inertness of lanthanide complexes is an important issue for their applicability in medical diagnosis since their products of dissociation, both free Ln^{III} ions and ligands, are toxic.[7] In vitro studies of the rate of dissociation reactions of Gd^{III} complexes may provide important information concerning their kinetic behaviour under physiological conditions. The dissociation of Ln-DOTA and Ln-DOTA-like complexes is very slow and generally occurs through a proton-assisted pathway without the involvement of endogenous metal ions like Zn^{II} and Cu^{II}.[45,55,56] The kinetic stabilities of Gd^{III} complexes are characterized either by the rates of their dissociation measured in 0.1 M HCl or by the rates of the transmetallation reaction, occurring in solutions with Zn^{II} and Cu^{II} or Eu^{III} ions.[42,45,55–59] To obtain information about the kinetic inertness of Gd^{III} complexes formed with this class of DO3A-like ligands bearing aminoethyl pendant arms, the metal-exchange reactions of Gd-**AE-DO3A** and Gd-**DMAE-DO3A** complexes with Cu^{II} were investigated at high Cu^{II} concentrations (10–20-fold excess) to guarantee the pseudo-first-order conditions. These reactions [Eq. (4)] were followed by spectrophotometry on the absorption band of the Cu-**AE-DO3A** and Cu-**AE-DO3A** at 300 nm in the pH range 3.2–5.2 (see the Supporting Information, Figures S13 and S14).

$$GdL + Cu^{2+} \rightleftharpoons CuL + Gd^{3+} \quad (4)$$

The definitions and equations used for the evaluation of the kinetic data are reported in the Supporting Information. The rate constants and the protonation constants characterizing the transmetallation reactions of Gd-**AE-DO3A** and Gd-**DMAE-DO3A** with Cu^{II} are listed in Table 7 and are compared with the corresponding values for Gd-DOTA and Gd-DO3A. The half-lives ($t_{1/2}$) of dissociation of Gd^{III} complexes calculated at pH 7.4 are included in Table 7.

Table 7. Rate and equilibrium constants and half-lives ($t_{1/2} = \ln 2/k_d$) of dissociation at pH 7.4 for the dissociation reactions of Gd-**AE-DO3A**, Gd-H**DMAE-DO3A**, Gd-**DO3A**$^-$ and Gd-**DOTA**$^-$ complexes (298 K).

	Gd-**AE-DO3A**	Gd-H**DMAE-DO3A**	Gd-**DO3A**[a]	Gd-**DOTA**[b]
ionic strength	0.1 M KCl	0.1 M KCl	0.1 M KCl	0.15 M NaCl
k_0 [s^{-1}]	$(-1\pm5)\times10^{-8}$	$(2\pm8)\times10^{-8}$	–	6.74×10^{-11}
k_1 [$M^{-1}s^{-1}$]	0.18 ± 0.03	$(4.3\pm0.3)\times10^{-2}$	2.3×10^{-2}	1.83×10^{-6}
k_2 [$M^{-1}s^{-1}$]	$(8.0\pm0.8)\times10^{2}$	–	–	–
K^H_{GdL}	8.1×10^{5} (pH-pot)	9.5×10^{7} (pH-pot)	115	14[c]
k_d [s^{-1}] pH 7.4	6.9×10^{-9}	1.7×10^{-9}	9.2×10^{-10}	7.3×10^{-14}
$t_{1/2}$ [h] pH 7.4	2.7×10^{4}	1.1×10^{5}	2.1×10^{5}	2.64×10^{9}

[a] Ref. [6]; [b] ref. [55]; [c] ref. [45].

Considering the pH range investigated (3.2–5.2) and the different speciation of the two GdL complexes, the transmetallation reactions occur between Cu^{II} ions and the monoprotonated Gd-H**DMAE-DO3A**, Gd-H**AE-DO3A** and the deprotonated Gd-**AE-DO3A** complexes. For Gd-**AE-DO3A** the reaction takes place through spontaneous dissociation of the deprotonated

(k_0) and monoprotonated (k_1) complexes, whereas the monoprotonated complex can also dissociate through the proton-assisted (k_2) pathway. On the other hand, for Gd-**DMAE-DO3A**, k_0 and k_1 characterize the spontaneous and proton-assisted dissociation of the monoprotonated Gd-H**DMAE-DO3A** complex that predominates in this pH range. This behaviour is similar to Gd-DO3A and Gd-DOTA, in which k_0 and k_1 characterize the spontaneous and proton-assisted dissociation of GdL. For the direct comparison of the kinetic inertness, the dissociation half-lives ($t_{1/2}$, hours) of GdL were calculated for pH 7.4 by using the rate and protonation constants reported in Table 7. The data indicate that $t_{1/2}$ for Gd-**AE-DO3A** is 4-, 8-, and 10^5 times shorter than for Gd-H**DMAE-DO3A**, Gd-DO3A and Gd-DOTA complexes, respectively, whereas the dissociation rate for Gd-H**DMAE-DO3A** is only two times faster than that of Gd-DO3A. The interpretation of dissociation kinetic data is somehow similar to that reported for Gd-DOTA and Gd-DO3A.[42,45,55–57] The complex dissociation mechanism typically involves proton transfer from a protonated species to a ring nitrogen, causing the release of Gd^{III} from the macrocyclic cavity. The proton transfer occurs more likely in a less rigid complex (i.e., Ln-DO3A), which can dissociate much faster than Ln-DOTA.[42,45,55–57] We have already assumed that the protonation of Gd-**AE-DO3A** and Gd-**DMAE-DO3A** takes place at the amino group of the pendant arm, so the resulting monoprotonated complexes highly resemble Gd-DO3A. Moreover, the faster dissociation of Gd-H**AE-DO3A** and Gd-H**DMAE-DO3A** complexes with respect to Gd-DO3A can be explained by the easier proton transfer mediated by the protonated pendant amino group. The lower basicity of the aminoethyl pendant arm than the dimethylaminoethyl is responsible for the lower kinetic inertness of Gd-H**AE-DO3A** since the conjugated acid transfers more efficiently the proton to the ring nitrogen. Finally, it is noteworthy that the $t_{1/2}$ values of Gd-**AE-DO3A** and Gd-H**DMAE-DO3A** are much higher than the half-lives of dissociation of the open-chain complexes, Gd-DTPA-BMA or Gd-DTPA (DTPA = diethylenetriamine-*N*,*N*,*N*′,*N*″,*N*″-pentaacetic acid; DTPA-BMA = diethylenetriamine-*N*,*N*,*N*′,*N*″,*N*″-pentaacetic acid bis-methylamide) ($t_{1/2}$ = 50 h and 305 h, respectively).[55]

Conclusion

The physicochemical properties of a series of aminoethyl macrocyclic complexes were comprehensively investigated with a multi-technique approach. The focus of this work was to explore solution behaviour and the potential of such complexes as pH-responsive MRI T_1 contrast agents. In particular, the increased substitution on the pendant amino group, passing from a primary amine to a tertiary one, was found to affect several characteristics of the complexes due to increased steric hindrance and to higher basicity of the metal-bound N-donor atom. The following changes were identified: 1) a shift to higher pH values of the pK_{aH} and larger Δr_{1p} from basic to acid pH; 2) structural modification of the complexes and presence of equilibria between differently hydrated species; 3) faster water-exchange rates when the amino group is coordinated to the metal centre; 4) lower total basicity of the ligands; 5) weaker coordination of the amino group to the metal ion; 6) higher kinetic inertness.

The behaviour of the protonated complexes was also investigated in detail, highlighting properties different from those of the simple correspondent DO3A complexes. Therefore, it was shown that the protonated amine on the pendant arm influences both the relaxometric and kinetic properties probably through the formation of a network of hydrogen bonds between the ammonium ion and the coordinated water molecule. This was mirrored by experimental evidence of both water-exchange rate reduction and faster dissociation of the Gd^{III} complex. An unusual mechanism for complex kinetic formation was proposed, which involves a second-order dependence of the rate constant on [OH^-] explained by the action of the amine as general base in the deprotonation and rearrangement steps.

Overall, this class of ligands constitutes a promising platform for developing new pH-sensitive probes. A better understanding of the effect of amine N-substitution was gained. Moreover, the possibility to insert different alkyl groups on the pendant amine can be exploited to prepare a library of compounds useful: 1) to increase the relaxivity variation in response to pH through amplification procedures such as anchoring or encapsulation into nanoparticles or protein interaction; 2) eventually to link the relaxivity change to the concentration of the complex through the preparation of dual imaging reporters.

Acknowledgements

This research was supported by the European Union and the State of Hungary, co-financed by the European Social Fund in the framework of TÁMOP 4.2.4. A/2-11-1-2012-0001 "National Excellence Program" (grant no.: A2-MZPD-12-0038; Z.B.); the Italy-Hungary Intergovernmental S&T Cooperation Program (HU11MO2-TET_10-1-2011-0202); the "Compagnia di San Paolo" (CSP-2012 NANOPROGLY Project). The research was also supported by the EU and co-financed by the European Social Fund under the project ENVIKUT (grant no.:TÁMOP-4.2.2.A-11/1/KONV-2012-0043) (A.F.). This study was performed under the auspices of EU-COST Action TD1004. We thank Fabio Carniato for his contribute in luminescence lifetime measurements and Nikolett Gajdics for her help in the equilibrium and kinetic experiments.

Keywords: contrast agents · lanthanides · NMR spectroscopy · macrocyclic ligands · thermodynamics

[1] C. F. G. C. Geraldes, S. Laurent, *Contrast Media Mol. Imaging* **2009**, *4*, 1–23.

[2] a) S. Aime, M. Botta, M. Fasano, S. G. Crich, E. Terreno, *J. Biol. Inorg. Chem.* **1996**, *1*, 312–319; b) R. B. Lauffer, D. J. Parmelee, S. U. Dunham, H. S. Ouellet, R. P. Dolan, S. Witte, T. J. McMurry, R. C. Walovitch, *Radiology* **1998**, *207*, 529–538.

[3] A. Datta, K. N. Raymond, *Acc. Chem. Res.* **2009**, *42*, 938; b) S. Aime, L. Calabi, C. Cavallotti, E. Gianolio, G. B. Giovenzana, P. Losi, A. Maiocchi, G. Palmisano, M. Sisti, *Inorg. Chem.* **2004**, *43*, 7588.

[4] H. Kobayashi, M. W. Brechbiel, *Curr. Pharm. Biotechnol.* **2004**, *5*, 539–549.

[5] W. J. M. Mulder, G. J. Strijkers, G. A. F. Van Tilborg, D. P. Cormode, Z. A. Fayad, K. Nicolay, *Acc. Chem. Res.* **2009**, *42*, 904 – 914.
[6] a) R. B. Lauffer, *Chem. Rev.* **1987**, *87*, 901 – 927; b) P. Caravan, J. J. Ellison, T. J. McMurry, R. B. Lauffer, *Chem. Rev.* **1999**, *99*, 2293 – 2352; c) P. Hermann, J. Kotek, V. Kubíček, I. Lukeš, *Dalton Trans.* **2008**, 3027 – 3047.
[7] *The Chemistry of Contrast Agents in Medical Magnetic Resonance Imaging, 2nd ed.* (Eds.: A. Merbach, L. Helm, E. Toth), Wiley, New York, **2013**.
[8] a) P. Caravan, *Chem. Soc. Rev.* **2006**, *35*, 512 – 523; b) S. Aime, D. D. Castelli, S. G. Crich, E. Gianolio, E. Terreno, *Acc. Chem. Res.* **2009**, *42*, 822 – 831.
[9] a) H. S. Thomsen, S. K. Morcos, P. Dawson, *Clin. Radiol.* **2006**, *61*, 905; b) S. Aime, P. Caravan, *J. Magn. Res. Imaging* **2009**, *30*, 1259 – 1267.
[10] a) H.-S. Chong, K. Garmestani, L. H. Bryant Jr., M. W. Brechbiel, *J. Org. Chem.* **2001**, *66*, 7745 – 7750; b) Z. Baranyai, F. Uggeri, G. B. Giovenzana, A. Bényei, E. Brücher, S. Aime, *Chem. Eur. J.* **2009**, *15*, 1696 – 1705.
[11] S. Achilefu, *Chem. Rev.* **2010**, *110*, 2575 – 2578, and whole thematic issue.
[12] a) R. Hovland, C. Gløgard, A. J. Aasen, J. Klaveness, *J. Chem. Soc. Perkin Trans. 2* **2001**, 929 – 933; b) S. Aime, D. D. Castelli, E. Terreno, *Angew. Chem.* **2002**, *114*, 4510 – 4512; *Angew. Chem. Int. Ed.* **2002**, *41*, 4334 – 4336.
[13] S. Aime, M. Botta, E. Gianolio, E. Terreno, *Angew. Chem.* **2000**, *112*, 763 – 766; *Angew. Chem. Int. Ed.* **2000**, *39*, 747 – 750.
[14] S. Zhang, R. Trokowski, A. D. Sherry, *J. Am. Chem. Soc.* **2003**, *125*, 15288 – 15289.
[15] E. L. Que, C. J. Chang, *Chem. Soc. Rev.* **2010**, *39*, 51 – 60.
[16] a) A. Louie, H. M. Huber, E. T. Ahrens, U. Rothbacher, R. Moats, R. E. Jacobs, S. E. Fraser, T. J. Meade, *Nat. Biotechnol.* **2000**, *18*, 321 – 325; b) B. Yoo, M. D. Pagel, *J. Am. Chem. Soc.* **2006**, *128*, 14302 – 14303.
[17] R. J. Gillies, N. Raghunand, M. L. Garcia-Martin, R. A. Gatenby, *IEEE Eng. Med. Biol. Mag.* **2004**, *23*, 57 – 64.
[18] M. P. Lowe, D. Parker, O. Reany, S. Aime, M. Botta, G. Castellano, E. Gianolio, R. Pagliarin, *J. Am. Chem. Soc.* **2001**, *123*, 7601 – 7609.
[19] S. Aime, M. Botta, S. G. Crich, G. Giovenzana, G. Palmisano, M. Sisti, *Chem. Commun.* **1999**, 1577 – 1578.
[20] a) S. Viswanathan, Z. Kovacs, K. N. Green, S. J. Ratnakar, A. D. Sherry, *Chem. Rev.* **2010**, *110*, 2960 – 3018; b) S. R. Zhang, M. Merritt, D. E. Woessner, R. E. Lenkiski, A. D. Sherry, *Acc. Chem. Res.* **2003**, *36*, 783 – 790.
[21] a) S. Zhang, K. Wu, A. D. Sherry, *Angew. Chem.* **1999**, *111*, 3382 – 3384; *Angew. Chem. Int. Ed.* **1999**, *38*, 3192 – 3194; b) D. L. Longo, W. Dastrù, G. Digilio, J. Kneupp, S. Langereis, S. Lanzardo, S. Prestigio, O. Steinbach, E. Terreno, F. Uggeri, S. Aime, *Magn. Reson. Chem.* **2011**, *65*, 202 – 211.
[22] G. B. Giovenzana, R. Negri, G. A. Rolla, L. Tei, *Eur. J. Inorg. Chem.* **2012**, 2035 – 2039.
[23] T. Krchová, J. Kotek, D. Jirák, J. Havlíčková, I. Císařová, P. Hermann, *Dalton Trans.* **2013**, *42*, 15735 – 15747.
[24] A. K. Mishra, J.-F. Chatal, *New J. Chem.* **2001**, *25*, 336 – 339.
[25] D. A. Moore, *Org. Synth.* **2008**, *85*, 10 – 14.
[26] a) J. I. Bruce, R. S. Dickins, L. J. Govenlock, T. Gunnlangsson, S. Lopinski, M. P. Lowe, D. Parker, J. J. B. Perry, S. Aime, M. Botta, *J. Am. Chem. Soc.* **2000**, *122*, 9674; b) L. Burai, R. Kiraly, E. Toth, E. Brucher, *Magn. Reson. Imaging* **1997**, *38*, 146.
[27] A. Beeby, I. M. Clarkson, R. S. Dickins, S. Faulkner, D. Parker, L. Royle, A. S. de Sousa, J. A. G. Williams, M. Woods, *J. Chem. Soc. Perkin Trans. 2* **1999**, 493 – 503.
[28] S. Aime, M. Botta, G. Ermondi, *Inorg. Chem.* **1992**, *31*, 4291 – 4299.
[29] S. Hoeft, K. Roth, *Chem. Ber.* **1993**, *126*, 869 – 873.
[30] V. Jacques, F. Desreux, *Inorg. Chem.* **1994**, *33*, 4048.
[31] S. Aime, M. Botta, M. Fasano, M. P. M. Marques, C. F. G. C. Geraldes, D. Pubanz, A. E. Merbach, *Inorg. Chem.* **1997**, *36*, 2059 – 2068.
[32] S. Aime, M. Botta, D. Parker, J. A. G. Williams, *J. Chem. Soc. Dalton Trans.* **1996**, 17 – 23.
[33] L. Banci, I. Bertini, C. Luchinat, *Nuclear and Electron Relaxation, The Magnetic Nucleus-Unpaired Electron Coupling in Solution*, VCH, Weinheim, **1991**; N. Bloembergen, L. O. Morgan, *J. Chem. Phys.* **1961**, *34*, 842.
[34] L. P. Hwang, J. H. Freed, *J. Chem. Phys.* **1975**, *63*, 4017; J. H. Freed, *J. Chem. Phys.* **1978**, *68*, 4034.
[35] T. J. Swift, R. E. J. Connick, *J. Chem. Phys.* **1962**, *37*, 307 – 312; D. H. Powell, O. M. Ni Dhubhghaill, D. Pubanz, L. Helm, Y. S. Lebedev, W. Schlaepfer, A. E. Merbach, *J. Am. Chem. Soc.* **1996**, *118*, 9333.
[36] S. Aime, M. Botta, S. G. Crich, G. B. Giovenzana, R. Pagliarin, M. Sisti, E. Terreno, *Magn. Reson. Chem.* **1998**, *36*, S200.
[37] L. Tei, G. Gugliotta, Z. Baranyai, M. Botta, *Dalton Trans.* **2009**, 9712 – 9714.
[38] M. Botta, S. Aime, A. Barge, G. Bobba, R. S. Dickins, D. Parker, E. Terreno, *Chem. Eur. J.* **2003**, *9*, 2102 – 2109.
[39] A. L. Thompson, D. Parker, D. A. Fulton, J. A. K. Howard, S. U. Pandya, H. Puschmann, K. Senanayake, P. A. Stenson, A. Badari, M. Botta, S. Avedano, S. Aime, *Dalton Trans.* **2006**, 5605 – 5616.
[40] M. Woods, M. Botta, S. Avedano, J. Wang, A. D. Sherry, *Dalton Trans.* **2005**, 3829 – 3837.
[41] J. F. Desreux, E. Merciny, M. F. Lincoln, *Inorg. Chem.* **1981**, *20*, 987.
[42] A. Takács, R. Napolitano, M. Purgel, A. Cs. Bényei, L. Zékány, E. Brücher, I. Tóth, Zs. Baranyai, S. Aime, *Inorg. Chem.* **2014**, submitted.
[43] A. Bianchi, L. Calabi, C. Giorgi, P. Losi, P. Mariani, P. Paoli, P. Rossi, B. Valtancoli, M. Virtuani, *J. Chem. Soc. Dalton Trans.* **2000**, 697.
[44] A. E. Martell, R. M. Smith, *Critical Stability Constants, Vol. 4*, Plenum, New York, **1974**.
[45] É. Tóth, E. Brücher, I. Lázár, I. Tóth, *Inorg. Chem.* **1994**, *33*, 4070.
[46] S. L. Wu, W. D. Horrocks, *Inorg. Chem.* **1995**, *34*, 3724.
[47] J. Moreau, E. Guillon, J. C. Pierrard, J. Rimbault, M. Port, M. Aplincourt, *Chem. Eur. J.* **2004**, *10*, 5218.
[48] W. P. Cacheris, S. K. Niekle, A. D. Sherry, *Inorg. Chem.* **1987**, *26*, 958.
[49] E. Brücher, G. Laurenczy, Z. S. Makra, *Inorg. Chim. Acta* **1987**, *139*, 141.
[50] X. Wang, T. Jin, V. Comblin, A. Lopez-Mut, E. Merciny, J. F. Desreux, *Inorg. Chem.* **1992**, *31*, 1095.
[51] K. Kumar, M. F. Tweedle, *Inorg. Chem.* **1993**, *32*, 4193.
[52] L. Burai, I. Fabian, R. Kiraly, E. Szilagyi, E. Brücher, *J. Chem. Soc. Dalton Trans.* **1998**, 243.
[53] E. Szilágyi, É. Tóth, Z. Kovács, J. Platzek, B. Radüchel, E. Brücher, *Inorg. Chim. Acta* **2000**, *298*, 226.
[54] F. K. Kálmán, PhD Dissertation, University of Debrecen, **2007**.
[55] Z. Baranyai, Z. Palinkas, F. Uggeri, A. Maiocchi, S. Aime, E. Brucher, *Chem. Eur. J.* **2012**, *18*, 16426.
[56] É. Tóth, R. Kiraly, J. Platzek, B. Raduchel, E. Brücher, *Inorg. Chim. Acta* **1996**, *249*, 191.
[57] P. Wedeking, K. Kumar, M. F. Tweedle, *Magn. Reson. Imaging* **1992**, *10*, 641.
[58] L. Sarka, L. Burai, E. Brücher, *Chem. Eur. J.* **2000**, *6*, 719.
[59] L. Sarka, L. Burai, R. Kiraly, L. Zekany, E. Brücher, *J. Inorg. Biochem.* **2002**, *91*, 320.
[60] K. Kumar, T. Jin, X. Wang, J. F. Desreux, M. F. Tweedle, *Inorg. Chem.* **1994**, *33*, 3823.
[61] H. M. Irving, M. G. Miles, L. Pettit, *Anal. Chim. Acta* **1967**, *38*, 475 – 488.
[62] L. Zékány, I. Nagypál, in *Computational Method for Determination of Formation Constants* (Ed.: D. J. Legett), Plenum, New York, **1985**, p. 291.

Received: October 16, 2013
Published online on February 7, 2014

